Journal of Zhejiang University-SCIENCE C (Computers & Electronics)
ISSN 1869-1951 (Print); ISSN 1869-196X (Online)
www.zju.edu.cn/jzus; www.springerlink.com
E-mail: jzus@zju.edu.cn

A numerical local orthogonal transform method for stratified waveguides*

Peng LI[1,2], Wei-zhou ZHONG[†‡1], Guo-sheng LI[3], Zhi-hua CHEN[4]

([1]*School of Economics and Finance, Xi'an Jiaotong University, Xi'an 710061, China*)

([2]*Department of Mathematics, North China University of Water Conservancy and Electric Power, Zhengzhou 450045, China*)

([3]*Department of Mathematics, Zhongyuan University of Technology, Zhengzhou 450007, China*)

([4]*Science Department, Zhijiang College of Zhejiang University of Technology, Hangzhou 310027, China*)

E-mail: weizhou@mail.xjtu.edu.cn

Received Nov. 29, 2009; Revision accepted Mar. 29, 2010; Crosschecked Sept. 6, 2010

Abstract: Flattening of the interfaces is necessary in computing wave propagation along stratified waveguides in large range step sizes while using marching methods. When the supposition that there exists one horizontal straight line in two adjacent interfaces does not hold, the previously suggested local orthogonal transform method with an analytical formulation is not feasible. This paper presents a numerical coordinate transform and an equation transform to perform the transforms numerically for waveguides without satisfying the supposition. The boundary value problem is then reduced to an initial value problem by one-way reformulation based on the Dirichlet-to-Neumann (DtN) map. This method is applicable in solving long-range wave propagation problems in slowly varying waveguides with a multilayered medium structure.

Key words: Helmholtz equation, Local orthogonal transform, Dirichlet-to-Neumann (DtN) reformulation, Marching method, Internal interface

doi:10.1631/jzus.C0910732 **Document code:** A **CLC number:** O29; O42

1 Introduction

A direct numerical computation can be very time consuming for small scale wave propagation problems. Common numerical methods, such as the finite difference method and the finite element method, lead to huge linear systems, which are also nonsymmetric and indefinite. Thus, it is hard to solve them. The coupled mode method (Jensen *et al.*, 1994) and some approximate methods (Tarppet, 1977; Fishman, 1993; Lee and Pierce, 1995; Lu and McLaughlin, 1996; Fishman *et al.*, 1997; Lu, 1999) based on exact one-way reformulation are popular because of their high efficiency in treating such problems; however, these numerical studies are usually confined to waveguides with flat boundaries or interfaces. Even though these methods can be applied to waveguides with a curved boundary if the 'staircase' approximation is used, they often result in marching in a very small range step. Many numerical methods have been developed to avoid the crude 'staircase' approximation. For example, the approach of Abrahamsson and Kreiss (1994) and Larsson and Abrahamsson (1998) uses a conformal mapping which keeps the governing equation in a very simple form. However, in general, the conformal mapping is global and requires much effort for its calculation, especially

‡ Corresponding author

* Project supported by the Program for New Century Excellent Talents in University (No. NCET-08-0450), the 985 II of Xi'an Jiaotong University, and the High Talented Person Scientific Research Start Project of North China University of Water Resources and Electric Power (No. 003001)

when the waveguide is very long and the boundaries (or interfaces) are complicated.

Local orthogonal transform (Lu *et al.*, 2001; Zhu and Lu, 2002) is an efficient method for flattening one curved bottom or interface and reducing the normal derivative at the interface or bottom to only the partial derivative in the transverse variable. Furthermore, the transformed governing equation does not involve the cross derivative term, and thus it is possible to be solved by some marching methods. For waveguides with at least two internal interfaces and satisfying the divisible assumption that there is a horizontal straight line between two adjacent interfaces, we have developed a local orthogonal coordinate transform and derived an 'improved Helmholtz equation' with two flat interfaces (Zhu and Li, 2007; 2008). Since the local orthogonal transforms are generally in an analytical form, we call it the analytical local orthogonal transform method (ALOTM). As mentioned above, the divisible assumption is not always valid practically, and a numerical local orthogonal transform method (NLOTM) that removes the divisible requirement would be very useful and applicable.

There are many recent publications (Nilsson, 2002; Andersson, 2008; 2009) using conformal mapping methods built on the modified Schwarz-Christoffel mapping for bent acoustic waveguides. Efficient numerical methods for conformal mappings of waveguides have also been developed (Andersson, 2008; 2009) to handle problems where the variations in geometry are found in a large proportion of the waveguide. Although these methods can be used to remove the divisible assumption required by previous versions of the local orthogonal transform methods and are competitive for medium bounded regions when the boundaries contain vertices or when parts of the boundaries are straight lines, they are far from efficient for an unbounded or large-scale region with boundary curves or interfaces that do not approach infinity as a straight line (Andersson, 2008). Therefore, NLOTM can be implemented with the marching processing and accordingly provides more computational efficiency for large-scale range-dependent waveguides. The NLOTM provides a framework for implementing some marching methods in waveguides with slowly varying curved interfaces. Furthermore, due to the fact that the Cauchy problem (Delillo *et al.*, 2001; Marin *et al.*, 2003; Marin, 2005; Jin and Zheng, 2006; Jin and Marin, 2008) has become an interesting research area in inverse problems in recent years, if the incident waves need to be reconstructed in large-scale stratified waveguides (Li *et al.*, 2008), the NLOTM can be used to flatten the curved interfaces or boundaries and is important for the computation involved with a large range step size.

2 Basic equation

In ocean acoustic applications, waves are allowed to travel large distances in the horizontal direction in this multilayered media where the surface can be seen as even, and the bottom is composed of multilayered media. The interfaces between two adjoint layers are usually curved. The range distance L is much larger than the typical wavelength. The depth D is also larger than the wavelength but much smaller than L. This typical structure is very common in acoustics, electro-magnetism, seismic migration, and some other applications.

Consider the two-dimensional (2D) Helmholtz equation in a typical ocean surrounding with two curved interfaces

$$u_{xx}+u_{zz}+\kappa^2(x,z)u=0 \tag{1}$$

for $-\infty<x<+\infty$, $0<z<D_1$, where the first layer with density ρ_1 is located in $0<z<h_1(x)$, and the second layer with density ρ_2 is located in $h_1(x)<z<h_2(x)$, and the third layer with density ρ_3 is located in $h_2(x)<z<D_1$. The interfaces are two curves $z=h_1(x)$ and $z=h_2(x)$, where $D_1>1$, $L\gg D_1\gg 1/k$, u represents the Fourier transform of acoustic pressure, and κ is called the wavenumber. We also suppose that the problem is range independent (i.e., wavenumber and interfaces are independent of x) for $x\leqslant 0$ and $x\geqslant L$, that is

$$h_1(x)=\begin{cases} h_{1,0}, & x\leqslant 0,\\ h_{1,\infty}, & x\geqslant L,\end{cases}\quad h_2(x)=\begin{cases} h_{2,0}, & x\leqslant 0,\\ h_{2,\infty}, & x\geqslant L,\end{cases}$$

$$\kappa(x,z)=\begin{cases} \kappa_0(z), & x\leqslant 0,\\ \kappa_\infty(z), & x\geqslant L.\end{cases}$$

The boundary conditions on the top and the bottom are supposed to be $u\big|_{z=0}=0$ and $u\big|_{z=D_1}=$

0. The interface conditions are as follows:

$$\begin{cases} \lim\limits_{z\to h_1(x)^-} u(x,z) = \lim\limits_{z\to h_1(x)^+} u(x,z), \\ \dfrac{1}{\rho_1}\lim\limits_{z\to h_1(x)^-} \dfrac{\partial u(x,z)}{\partial \boldsymbol{n}} = \dfrac{1}{\rho_2}\lim\limits_{z\to h_1(x)^+} \dfrac{\partial u(x,z)}{\partial \boldsymbol{n}}, \\ \lim\limits_{z\to h_2(x)^-} u(x,z) = \lim\limits_{z\to h_2(x)^+} u(x,z), \\ \dfrac{1}{\rho_2}\lim\limits_{z\to h_2(x)^-} \dfrac{\partial u(x,z)}{\partial \boldsymbol{n}} = \dfrac{1}{\rho_3}\lim\limits_{z\to h_2(x)^+} \dfrac{\partial u(x,z)}{\partial \boldsymbol{n}}, \end{cases}$$

where $\boldsymbol{n}$ is a normal vector of the interface $z=h_1(x)$ or $z=h_2(x)$ (Fig. 1).

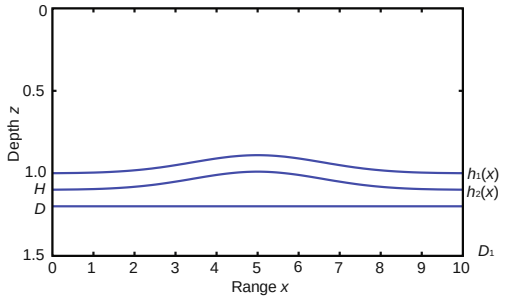

Fig. 1 Sketch map of waveguide with curved internal interfaces

Here we shall concentrate on solving the equation for $0 \leqslant x \leqslant L$ since the Helmholtz equation can be easily solved by a separable variable method for $x \leqslant 0$ or $x \geqslant L$. Supposing there are no waves coming from $+\infty$, we have the exact boundary condition (radiation condition) at $x=L$, $u_x = \mathrm{i}\sqrt{\partial_z^2 + \kappa_\infty^2(z)}u$, where $\mathrm{i}=\sqrt{-1}$. The simplest boundary condition at $x=0$ is imposed as $u=u_0(z)$ for a given function $u_0(z)$.

For simple derivation and illustration, our method is developed for the waveguides with only two curved internal interfaces, but it can be extended to waveguides with more interfaces. In this method, we remove the divisible assumption and consider a general acoustical waveguide: there may be no horizontal straight line $z=D_0$ between two adjoint interfaces $h_1(x)$ and $h_2(x)$. We suppose that a unique solution exists for Eq. (1) with the boundary and interface conditions.

3 Local orthogonal transform

To avoid constricting the coordinate net into a narrow coordinate net in the (x,z) plane, we further divide the layer below $z=h_2(x)$ into two sub-layers: $h_2(x) < z < D$ and $D < z < D_1$ with the added interface $z=D$. The detailed transform scheme to flatten the curved interfaces

$$\begin{cases} \hat{x} = f(x,z), \\ \hat{z} = g(x,z), \end{cases}$$

are as follows:

$$\frac{\partial f}{\partial x}\cdot\frac{\partial g}{\partial x} + \frac{\partial f}{\partial z}\cdot\frac{\partial g}{\partial z} = 0,$$

where the function f is to be determined according to the orthogonal condition.

1. The first layer $0 \leqslant z \leqslant h_1(x)$ in a medium with density ρ_1 (Zhu and Lu, 2002). Let

$$\begin{cases} \hat{x} = f(x,z), \\ \hat{z} = g(x,z) = z/h(x), \end{cases}$$

satisfy $\{(x,z)|0 \leqslant x \leqslant L,\ 0 \leqslant z \leqslant h_1(x)\} \xleftrightarrow{f,g} \{(\hat{x},\hat{z})|\ 0 \leqslant x \leqslant L,\ 0 \leqslant \hat{z} \leqslant 1\}$.

2. The second layer $h_1(x) \leqslant z \leqslant h_2(x)$ in a medium with density ρ_2 (Zhu and Lu, 2002). Let

$$\begin{cases} \hat{x} = f(x,z), \\ \hat{z} = g(x,z) = \dfrac{z-h_1(x)}{h_2(x)-h_1(x)}\cdot(H-1)+1, \end{cases}$$

satisfy $\{(x,z)|0 \leqslant x \leqslant L,\ h_1(x) \leqslant z \leqslant h_2(x)\} \xleftrightarrow{f,g} \{(\hat{x},\hat{z})|0 \leqslant x \leqslant L,\ 1 \leqslant \hat{z} \leqslant H\}$.

3. The third layer $h_2(x) \leqslant z \leqslant D$ in a medium with density ρ_3. Let

$$\begin{cases} \hat{x} = f(x,z), \\ \hat{z} = g(x,z) = \dfrac{z-D}{D-h_2(x)}\cdot(D-H)+D, \end{cases}$$

satisfy $\{(x,z)|0 \leqslant x \leqslant L,\ h_2(x) \leqslant z \leqslant D\} \xleftrightarrow{f,g} \{(\hat{x},\hat{z})|0 \leqslant \hat{x} \leqslant L,\ H \leqslant \hat{z} \leqslant D\}$.

4. The fourth layer $D \leqslant \hat{z} \leqslant D_1$ in a medium with density ρ_3. Let

$$\begin{cases} \hat{x} = f(x,D), \\ \hat{z} = g(x,z) = z, \end{cases}$$

satisfy $\{(x,z)|0 \leqslant x \leqslant L,\ D \leqslant z \leqslant D_1\} \xleftrightarrow{f,g} \{(\hat{x},\hat{z})|0 \leqslant \hat{x} \leqslant L,\ D \leqslant \hat{z} \leqslant D_1\}$.

4 Equation transformation

Because Eq. (1) is expected to be transformed as

$$V_{\hat{x}\hat{x}} + \alpha(\hat{x},\hat{z})V_{\hat{z}\hat{z}} + \beta(\hat{x},\hat{z})V_{\hat{z}} + \gamma(\hat{x},\hat{z})V = 0, \quad (2)$$

we let $u(x,z)=W(x,z)\cdot V(x,z)$ and the coefficient of the $V_{\hat{x}}$ be zero in order to remove $V_{\hat{x}}$. Then $W(x,z)$ is governed by $2W_zf_z+Wf_{zz}+2W_xf_x+Wf_{xx}=0$ (Zhu and Lu, 2002). Coefficients of Eq. (2) are obtained as follows:

$$\begin{cases}\alpha(\hat{x},\hat{z})=\dfrac{g_z^2+g_x^2}{f_z^2+f_x^2},\\[2ex]\beta(\hat{x},\hat{z})=\dfrac{2W_zg_z+Wg_{zz}+2W_xg_x+Wg_{xx}}{W(f_z^2+f_x^2)},\\[2ex]\gamma(\hat{x},\hat{z})=\dfrac{W_{xx}+W_{zz}+\kappa^2W}{W(f_z^2+f_x^2)}.\end{cases}\tag{3}$$

To compute the coefficients of the transformed Eq. (3) in the multilayered waveguide, the numerical algorithm considers two aspects: (1) coordinate transformation, i.e., the computation of f,g, and its corresponding partial derivatives; (2) equation transformation, i.e., the computation of $W(x,z)$ and its corresponding partial derivatives.

4.1 Coordinate transformation

Coordinate transforms should be consistent with the operator marching. Let the marching computation come to the position at $\hat{x}=\hat{x}_j$, and f,g be computed on the coordinate line $\hat{x}_j=f(x,z)$. Here, we also compute its relative derivatives, which will be used later in the computation of the equation transformation.

Differentiating with respect to z along $\hat{x}_j=f(x,z)$ gives

$$f_z+f_x\frac{\mathrm{d}x}{\mathrm{d}z}=0;$$

that is,

$$\frac{\mathrm{d}x}{\mathrm{d}z}=-\frac{f_z}{f_x}.$$

Since the transform is required to be orthogonal, that is

$$\frac{\partial f}{\partial x}\cdot\frac{\partial g}{\partial x}+\frac{\partial f}{\partial z}\cdot\frac{\partial g}{\partial z}=0,$$

we have

$$-\frac{f_z}{f_x}=\frac{g_x}{g_z}.$$

Hence, the equation coordinates curve $\hat{x}_j=f(x,z)$ satisfies

$$\frac{\mathrm{d}x}{\mathrm{d}z}=F(z,x)\triangleq\frac{g_x}{g_z},$$

whose analytical formulation can be derived in every layer:

$$\frac{\mathrm{d}x}{\mathrm{d}z}=F(z,x)=$$

$$\begin{cases}-\dfrac{h_1'(x)}{h_1(x)}z, & 0\leqslant z\leqslant h_1(x),\\[2ex]-\dfrac{1}{h_2(x)-h_1(x)}[h_2'(x)(h_2(x)-h_1(x))+(z-h_2(x))(h_2'(x)-h_1'(x))], & h_1(x)\leqslant z\leqslant h_2(x),\\[2ex]\dfrac{h_2'(x)}{D-h_2(x)}(z-D), & h_2(x)\leqslant z\leqslant D,\\[2ex]0, & D\leqslant z\leqslant D_1,\end{cases}\tag{4}$$

with the initial condition $x(0)=\hat{x}_j$.

The classical Runge-Kutta method of solving ordinary differential equations (ODEs) can be applied to calculate the physical coordinate from the computing coordinate along $\hat{x}=\hat{x}_j$.

From a computed discrete point-set $\{(x_i,z_i)|1\leqslant i\leqslant M\}$ of physical coordinates, we can reformulate

$$\begin{cases}x=m(\hat{x},\hat{z}),\\z=n(\hat{x},\hat{z}),\end{cases}\tag{5}$$

by some interpolation methods at $\hat{x}=\hat{x}_j$, which is the inverse function of

$$\begin{cases}\hat{x}=f(x,z),\\\hat{z}=g(x,z).\end{cases}$$

Details are omitted here as they can be found in many basic textbooks concerning numerical analysis.

Differentiating partially to $\hat{x}$ and $\hat{z}$ respectively along $\hat{x}=f(x,z)$ gives $f_{\hat{x}}=1$, $f_{\hat{z}}=0$, which can be written as

$$\begin{cases}f_xm_{\hat{x}}+f_zn_{\hat{x}}=1,\\f_xm_{\hat{z}}+f_zn_{\hat{z}}=0.\end{cases}\tag{6}$$

Then we have

$$\begin{cases}f_x=-\dfrac{n_{\hat{z}}}{n_{\hat{x}}m_{\hat{z}}-n_{\hat{z}}m_{\hat{x}}},\\[2ex]f_z=\dfrac{m_{\hat{z}}}{n_{\hat{x}}m_{\hat{z}}-n_{\hat{z}}m_{\hat{x}}}.\end{cases}\tag{7}$$

From Eq. (7), we obtain

$$\begin{cases}f_{xx}=(f_x)_{\hat{x}}f_x+(f_x)_{\hat{z}}g_x,\\f_{zz}=(f_z)_{\hat{x}}f_z+(f_z)_{\hat{z}}g_z,\end{cases}\tag{8}$$

where

$$(f_x)_{\hat{x}} = \frac{-1}{(n_{\hat{x}}m_{\hat{z}} - n_{\hat{z}}m_{\hat{x}})^2} \cdot \big[n_{\hat{z}\hat{x}}(n_{\hat{x}}m_{\hat{z}} - n_{\hat{z}}m_{\hat{x}}) - n_{\hat{z}}(n_{\hat{x}\hat{x}}m_{\hat{z}} + n_{\hat{x}}m_{\hat{x}\hat{z}} - n_{\hat{x}\hat{z}}m_{\hat{x}} - n_{\hat{z}}m_{\hat{x}\hat{x}})\big].$$

$(f_x)_{\hat{z}}, (f_z)_{\hat{x}}, (f_z)_{\hat{z}}$ can be computed in the same way, and we omit the details here.

Once $m_{\hat{z}}, n_{\hat{z}}, m_{\hat{z}\hat{z}}, n_{\hat{z}\hat{z}}$ and $m_{\hat{x}}, n_{\hat{x}}, m_{\hat{x}\hat{x}}, n_{\hat{x}\hat{x}}$ are computed, f_x, f_z, f_{xx}, f_{zz} can be obtained numerically according to Eqs. (7) and (8). In this work, $m_{\hat{z}}, n_{\hat{z}}, m_{\hat{z}\hat{z}}, n_{\hat{z}\hat{z}}$ are computed separately in L_1 $(0 < \hat{z} < 1.0), L_2$ $(1.0 < \hat{z} < H), L_3$ $(H < \hat{z} < D)$, and L_4 $(D < \hat{z} < D_1)$ by the following three-point formulae with a properly selected step h:

$$P_{\hat{z}}(\hat{x}, \hat{z}_i) = \frac{-P(\hat{x}, \hat{z}_i - h) + P(\hat{x}, \hat{z}_i + h)}{2h}, \quad (9)$$

$$P_{\hat{z}\hat{z}}(\hat{x}, \hat{z}_i) = \frac{P(\hat{x}, \hat{z}_i - h) - 2P(\hat{x}, \hat{z}_i) + P(\hat{x}, \hat{z}_i + h)}{h^2}, \quad (10)$$

where h satisfies: if $\hat{z}_i \in L_j$ and $\hat{z}_{i+1} \in L_j$, then $\hat{z}_i \pm h \in L_j$ and $\hat{z}_i + h \leqslant \hat{z}_{i+1}$, with $j = 1, 2, 3, 4$. In general, if the step sizes for a discrete depth variable $\hat{z}$ are not very small or too large, we can directly use the function values on discretized points in each layer to compute the derivatives.

With respect to the computing of $m_{\hat{x}}, n_{\hat{x}}$, $m_{\hat{x}\hat{x}}, n_{\hat{x}\hat{x}}$ at $\hat{x} = \hat{x}_j$, the Runge-Kutta method is used to compute $m(\hat{x}, \hat{z}), n(\hat{x}, \hat{z})$ at $\hat{x} = \hat{x}_j - \delta, \hat{x} = \hat{x}_j, \hat{x} = \hat{x}_j + \delta$ for some properly selected $\delta > 0$, and then the derivatives with respect to $\hat{x}$ are approximated by the three-point numerical derivatives:

$$P_{\hat{x}}(\hat{x}_j, \hat{z}) = \frac{-P(\hat{x}_j - \delta, \hat{z}) + P(\hat{x}_j + \delta, \hat{z})}{2\delta}, \quad (11)$$

$$P_{\hat{x}\hat{x}}(\hat{x}_j, \hat{z}) = \frac{P(\hat{x}_j - \delta, \hat{z}) - 2P(\hat{x}_j, \hat{z}) + P(\hat{x}_j + \delta, \hat{z})}{\delta^2}. \quad (12)$$

Note here that the computing of numerical derivatives is not a stable process in that small changes in function values may cause large changes in the values of the corresponding derivatives. The selection of the optimal step sizes h and δ for numerical derivative is crucial for the coordinate transformation: too small a step size amplifies the side effects of the noise in original data; too large a step size weakens the accuracy in approximating a derivative. Theoretically, there is an optimal step size which balances the trade-off between numerical stability and accuracy. In general, for slowly varing waveguides, there exists a neighborhood of the optimal step size in which the numerical derivative can be computed exactly and stably. Thus, in practice, we need only to find one proper value from the neighborhood by some preliminary numerical tests, instead of computing the optimal one with more efforts.

4.2 Equation transformation

To obtain an equation transformation, the calculation of $W(x, z)$ and its corresponding partial derivatives are necessary. $W(x, z)$ is governed by

$$2W_z f_z + W f_{zz} + 2W_x f_x + W f_{xx} = 0. \quad (13)$$

At $(\hat{x}, \hat{z})$, substituting

$$W_x = W_{\hat{x}} f_x + W_{\hat{z}} g_x, \quad W_z = W_{\hat{x}} f_z + W_{\hat{z}} g_z \quad (14)$$

into Eq. (13) gives

$$2(f_x^2 + f_z^2)W_{\hat{x}} + 2(f_x g_x + f_z g_z)W_{\hat{z}} + (f_{xx} + f_{zz})W = 0, \quad (15)$$

which can be written as

$$W_{\hat{x}} = \theta W, \quad (16)$$

where $\theta = -\left.\dfrac{f_{xx} + f_{zz}}{2(f_x^2 + f_z^2)}\right|_{\hat{x}_{1/2}}$. Note that W can be seen as a function of $(\hat{x}, \hat{z})$ and also (x, z). We denote it by $W(\hat{x}, \hat{z})$ or $W(x, z)$ for simplicity in the following derivation. It is the same with θ.

Eq.(16) has the exact solution

$$W(\hat{x}) = W(L)\exp\left(\int_L^{\hat{x}} \theta(t)\mathrm{d}t\right), \quad (17)$$

which can be solved easily using some marching methods. The step formulation from $\hat{x}_1$ to $\hat{x}_0$ is used to represent the general step from $\hat{x}_{k+1}$ to $\hat{x}_k$:

$$W_1 \approx \mathrm{e}^{\theta\tau} W_0, \quad (18)$$

where $\tau = \hat{x}_1 - \hat{x}_0$, with the initial condition $W(L, \hat{z}) = 1$ $(0 \leq \hat{z} \leq D_1)$. For Eq. (17), supposing that $W(L, \hat{z})$ is polluted initial data and $W^*(L, \hat{z})$ is exact, and that $\theta(t)$ is computed and $\theta^*(t)$ is exact, we have the error propagating estimation as shown later. Note here that, we omit the variable $\hat{z}$ in some functions for simplicity in notation, such as $W(L, \hat{z}) \mapsto W(L), W(\hat{x}, \hat{z}) \mapsto W(\hat{x}), \theta(t, \hat{z}) \mapsto \theta(t)$.

Theorem 1 Let $\theta(t) - \theta^*(t) = e(t)$, and $W(\hat{x})$ and $W^*(\hat{x})$ be solutions of Eq. (16) corresponding to $\theta(t)$ and $\theta^*(t)$, respectively. Then we have

(1)

$$\frac{W(\hat{x})}{W^*(\hat{x})}=\exp\left(\int_L^{\hat{x}} e(t)\mathrm{d}t\right)\frac{W(L)}{W^*(L)}. \tag{19}$$

(2)

$$C_1\le\left|\frac{W(\hat{x})}{W^*(\hat{x})}\right|\le C_2, \tag{20}$$

with $C_1=\min\limits_{0\le\hat{x}<L}\left|\frac{W(L)}{W^*(L)}\cdot\exp\left(\int_L^{\hat{x}} e(t)\mathrm{d}t\right)\right|$ and $C_2=\max\limits_{0\le\hat{x}<L}\left|\frac{W(L)}{W^*(L)}\cdot\exp\left(\int_L^{\hat{x}} e(t)\mathrm{d}t\right)\right|$.

(3) Let $||e(t)||_\infty=c, W(L)\equiv W^*(L)$. For any $\varepsilon>0$, if

$$c<\min\left\{-\frac{1}{L}\ln(1-\varepsilon),\frac{1}{L}\ln(1+\varepsilon)\right\}, \tag{21}$$

then

$$\left|\left|\frac{W(\hat{x})}{W^*(\hat{x})}\right|-1\right|<\varepsilon. \tag{22}$$

Proof

(1) From Eq. (17), we have

$$W^*(\hat{x})=\exp\left(\int_L^{\hat{x}}\theta^*(t)\mathrm{d}t\right)W^*(L). \tag{23}$$

Eq. (23) dividing Eq. (17) gives

$$\begin{aligned}\frac{W(\hat{x})}{W^*(\hat{x})}&=\exp\left(\int_L^{\hat{x}}[\theta(t)-\theta^*(t)]\mathrm{d}t\right)\frac{W(L)}{W^*(L)}\\&=\exp\left(\int_L^{\hat{x}} e(t)\mathrm{d}t\right)\frac{W(L)}{W^*(L)},\end{aligned}$$

which is Eq. (19).

(2) Taking the absolute value of Eq. (19), we have

$$C_1\le\left|\frac{W(\hat{x})}{W^*(\hat{x})}\right|=\exp\left(\int_L^{\hat{x}} e(t)\mathrm{d}t\right)\left|\frac{W(L)}{W^*(L)}\right|\le C_2,$$

with $C_1=\min\limits_{0\le\hat{x}<L}\left|\frac{W(L)}{W^*(L)}\cdot\exp\left(\int_L^{\hat{x}} e(t)\mathrm{d}t\right)\right|$ and $C_2=\max\limits_{0\le\hat{x}<L}\left|\frac{W(L)}{W^*(L)}\cdot\exp\left(\int_L^{\hat{x}} e(t)\mathrm{d}t\right)\right|$.

(3) For $||e(t)||_\infty=c, W(L)\equiv W^*(L)$, from Eq. (20) we have

$$C_1\ge\min_{0\le\hat{x}<L}\exp\left(\int_L^{\hat{x}}||e(t)||_\infty\mathrm{d}t\right)$$

$$=\exp\left(\int_L^{\hat{x}} c\mathrm{d}t\right)\ge\exp\left(\int_L^{0} c\mathrm{d}t\right)=\mathrm{e}^{-Lc}. \tag{24}$$

and

$$C_2\le\max_{0\le\hat{x}<L}\exp\left(-\int_L^{\hat{x}}||e(t)||_\infty\mathrm{d}t\right)$$

$$=\exp\left(\int_L^{\hat{x}} c\mathrm{d}t\right)\le\exp\left(-\int_L^{0} c\mathrm{d}t\right)=\mathrm{e}^{Lc}. \tag{25}$$

Letting $\mathrm{e}^{-Lc}>1-\varepsilon$ and $\mathrm{e}^{Lc}<1+\varepsilon$, then from Eqs. (24) and (25) we have

$$1-\varepsilon<C_1\le\left|\frac{W(\hat{x})}{W^*(\hat{x})}\right|\le C_2<1+\varepsilon \tag{26}$$

if

$$c<\min\left\{-\frac{1}{L}\ln(1-\varepsilon),\frac{1}{L}\ln(1+\varepsilon)\right\}.$$

Thus, under the constraint Eq. (19), we have

$$-\varepsilon<\left|\frac{W(\hat{x})}{W^*(\hat{x})}\right|-1<\varepsilon;$$

that is,

$$\left|\left|\frac{W(\hat{x})}{W^*(\hat{x})}\right|-1\right|<\varepsilon.$$

Since there is no initial error in $W(L)$ with $W(L,\hat{z})\equiv W^*(L,\hat{z})\equiv 1$ $(0\le\hat{z}\le D_1)$, the deviations of $W(\hat{x})$ are completely determined by the errors $e(t)$, which arise from the calculation of $\theta(t)$, and Eq. (21) can be taken as a practical approximate estimate. If the accuracy of $\theta(t)$ can be controlled successfully, the accumulated errors for $W(\hat{x})$ will not be serious. For the slowly varied waveguides, $\theta(t)$ is also slowly varied and it is possible to control the accuracy and stability in numerical derivative computing. Furthermore, if the computed domain is very long and the errors are excessively accumulated, we can reset $W(\hat{x}',\hat{z})=1$ in some $\hat{x}=\hat{x}'$ where the interfaces and boundaries are flat in its neighborhood, since $W(\hat{x},\hat{z})$ satisfying Eq. (13) has a constant solution $W(\hat{x},\hat{z})\equiv 1$ in the area with flat interfaces and boundaries. The marching process can then be continued from the new starting point.

From Eq. (16), we have

$$W_{\hat{x}\hat{x}}=(W_{\hat{x}})_{\hat{x}}=(\theta W)_{\hat{x}}=\theta_{\hat{x}}W+\theta W_{\hat{x}}=(\theta_{\hat{x}}+\theta^2)W, \tag{27}$$

where $\theta_{\hat{x}}$ can be computed by Eq. (11). In this way, $W_{\hat{x}}$ and $W_{\hat{x}\hat{x}}$ can be computed from Eqs. (16) and (27).

To obtain the coefficients of Eq. (2) according to Eq. (3), we still need to compute $W_{\hat{z}}$ and $W_{\hat{z}\hat{z}}$ numerically. Once $W(\hat{x},\hat{z})$ at $\hat{x}=\hat{x}_j$ is computed, this can be approximated by the three-point numerical derivatives Eqs. (9) and (10) in L_1 $(0<\hat{z}<1.0), L_2$ $(1.0<\hat{z}<H), L_3$ $(H<\hat{z}<D)$, and L_4 $(D<\hat{z}<D_1)$, respectively. After $W_{\hat{x}}, W_{\hat{x}\hat{x}}, W_{\hat{z}}$, and $W_{\hat{z}\hat{z}}$ are computed, we have

$$\begin{cases} W_{xx}=W_{\hat{x}\hat{x}}f_x^2+2W_{\hat{x}\hat{z}}f_xg_x+W_{\hat{z}\hat{z}}g_x^2+W_{\hat{x}}f_{xx}+W_{\hat{z}}g_{xx}, \\ W_{zz}=W_{\hat{x}\hat{x}}f_z^2+2W_{\hat{x}\hat{z}}f_zg_z+W_{\hat{z}\hat{z}}g_z^2+W_{\hat{x}}f_{zz}+W_{\hat{z}}g_{zz}. \end{cases} \tag{28}$$

Then, one can compute the coefficients of the transformed Helmholtz equation (Eq. (2)) according to Eq. (3).

5 Interface conditions

For Eq. (2), the top and bottom boundary conditions are

$$V|_{\hat{z}=0}=0, \quad V|_{\hat{z}=D_1}=0. \tag{29}$$

The interface conditions between the first and the second layers (at $\hat{z}=1$) become

$$\begin{aligned} &(WV)|_{\hat{z}=1^-}=(WV)|_{\hat{z}=1^+}, \\ &\frac{1}{\rho_1}\left\{\tfrac{1}{2}[h_1'(x)W_x-W_z]V-W[h_1'(x)g_x-g_z]V_{\hat{z}}\right\}\Big|_{\hat{z}\to 1^-} \\ &=\frac{1}{\rho_2}\left\{\tfrac{1}{2}[h_1'(x)W_x-W_z]V-W[h_1'(x)g_x-g_z]V_{\hat{z}}\right\}\Big|_{\hat{z}\to 1^+}. \end{aligned} \tag{30}$$

The interface conditions between the third and the fourth layers (at $\hat{z}=H$) become

$$\begin{aligned} &(WV)|_{\hat{z}=H^-}=(WV)|_{\hat{z}=H^+}, \\ &\frac{1}{\rho_2}\left\{\tfrac{1}{2}[h_2'(x)W_x-W_z]V-W[h_2'(x)g_x-g_z]V_{\hat{z}}\right\}\Big|_{\hat{z}\to H^-} \\ &=\frac{1}{\rho_3}\left\{\tfrac{1}{2}[h_2'(x)W_x-W_z]V-W[h_2'(x)g_x-g_z]V_{\hat{z}}\right\}\Big|_{\hat{z}\to H^+}. \end{aligned} \tag{31}$$

The conditions at the interface between the fourth and the fifth layers (at $\hat{z}=D$) are

$$\begin{aligned} &WV|_{\hat{z}\to D^-}=WV|_{\hat{z}\to D^+}, \\ &-\tfrac{1}{2}W_zV+Wg_zV_{\hat{z}}\Big|_{\hat{z}\to D^-}=-\tfrac{1}{2}W_zV+Wg_zV_{\hat{z}}\Big|_{\hat{z}\to D^+}. \end{aligned} \tag{32}$$

6 Numerical examples

Range discretization and matrix approximation to the operator $\alpha(\hat{x},\hat{z})\partial_z^2+\beta(\hat{x},\hat{z})\partial_z+\gamma(\hat{x},\hat{z})$ are the same as those in Zhu and Lu (2002). We omit it in this paper for simplicity.

The NLOTM has been tested on a number of examples. We present four of them below. In the first example, for the layer between $h_1(x)$ and $h_2(x)$ which satisfies the divisible assumption, it can be solved by both the ALOTM and the NLOTM. The solution obtained by the NLOTM is compared with that of the ALOTM. The second to the fourth examples are situations without satisfying the divisible assumption solved using our new method.

Example 1 Let

$$\kappa=\begin{cases} 16, & 0<z<h_1(x), \\ 0.7\times 16, & h_1(x)<z<h_2(x), \\ 0.2\times 16, & h_2(x)<z<D_1, \end{cases}$$

with L=10, n=30, D_0=1.5, H=2.5, D=3, D_1=4, N=400, ρ_1=1, ρ_2=1.7, ρ_3=2.7, δ=0.025, $h_1(x)=1-\varepsilon_1\exp(-\sigma_1(x/L-0.5)^2)$, $h_2(x)=H-\varepsilon_2\exp(-\sigma_2(x/L-0.5)^2)$, $\varepsilon_1=\varepsilon_2=0.1$, $\sigma_1=\sigma_2=10$, $0\leqslant z\leqslant 4, 0\leqslant x\leqslant 10$, where N is the number of points to discretize the $\hat{z}$ variable, n is the number to truncate the $N\times N$ matrices that approximate the operators arising in the marching process (Zhu and Lu, 2002). Note that all the derivatives with respect to $\hat{z}$ are computed directly on the values of the discretizing points in Examples 1–4, and that h is a constant in each layer.

Here, $u(0,\hat{z})$ is given by the eigenfunction whose corresponding eigenvalue is the largest one at $x=L$ (Fig. 2). After flattening the two curved interfaces by the orthogonal transform we suggest, the marching scheme in Zhu and Lu (2002) can be implemented to compute the solution $u(\hat{x},\hat{z})$ at $\hat{x}=L$. The corresponding solution is shown in Fig. 3. With the ALOTM solutions acting as the 'exact' solutions, the relative error of Example 1 is 0.0384. As shown in Fig. 3, the real parts of $u(L,\hat{z})$ with range steps $\tau=1/8$ and $\tau=1/128$ fit closely, while the imaginary part has a slight discrepancy. The difference may come from: (1) errors from computing numerical derivatives, which suggests that a proper selection δ and control of the random error in computing derivatives are needed in a further study; (2) effects of the introduced additional interface conditions in the ALOTM, which results in different discretizations of deep variable $\hat{z}$ and corresponding different matrix approximations.

In Fig. 4, the NLOTM solution obtained with

$\delta = 0.025$ acts as the 'exact' solution and the relative error of the solution obtained with $\delta = 0.05$ is 0.0109. As shown in Fig. 4, the solutions obtained fit closely. The numerical test justifies the existence of neighborhood of the optimal step size. In practical computing, we need only to find one step size from the neighborhood instead of the optimal one. It is easy to verify that $\delta = 0.05$ is a rational step size for the numerical derivative computed under the error level of the current problems.

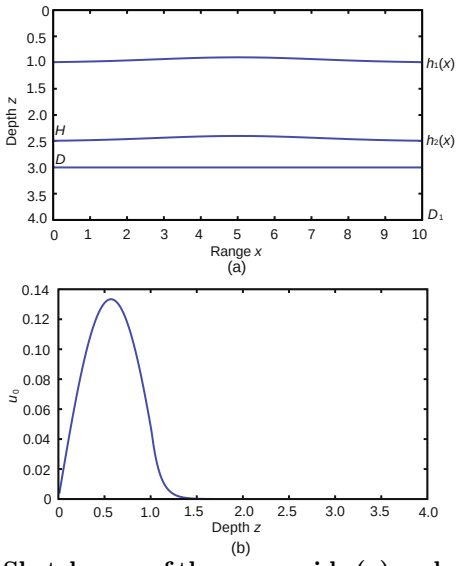

Fig. 2 Sketch map of the waveguide (a) and $u(0,z)$ (b) in Example 1

Example 2 Let

$$\kappa = \begin{cases} 16, & 0 < z < h_1(x), \\ 0.7 \times 16, & h_1(x) < z < h_2(x), \\ 0.2 \times 16, & h_2(x) < z < D_1, \end{cases}$$

with $L = 10$, $n = 30$, $H = 1.1$, $D = 1.2$, $D_1 = 1.5$, $N = 200$, $\rho_1 = 1$, $\rho_2 = 1.7$, $\rho_3 = 2.7$, $\delta = 0.05$, $h_1(x) = 1 - \varepsilon_1 \exp(-\sigma_1(x/L - 0.5)^2)$, $h_2(x) = H - \varepsilon_2 \exp(-\sigma_2(x/L - 0.5)^2)$, $\varepsilon_1 = \varepsilon_2 = 0.11$, $\sigma_1 = \sigma_2 = 2$, $0 \leqslant z \leqslant 1.5$, $0 \leqslant x \leqslant 10$.

Here, $u(0, \hat{z})$ is given by the eigenfunction whose corresponding eigenvalue is the second largest one at $x = L$ (Fig. 5). The corresponding solution at $x = L$ is shown in Fig. 6.

Example 3 Let

$$\kappa = \begin{cases} 16, & 0 < z < h_1(x), \\ 0.7 \times 16, & h_1(x) < z < h_2(x), \\ 0.2 \times 16, & h_2(x) < z < D_1, \end{cases}$$

with $L = 10$, $n = 30$, $H = 1.08$, $D = 1.2$, $D_1 = 1.5$, $N = 200$, $\rho_1 = 1$, $\rho_2 = 1.7$, $\rho_3 = 2.7$, $\delta = 0.05$,

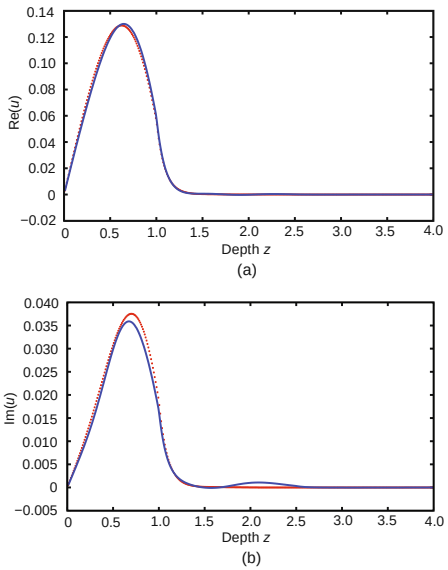

Fig. 3 Comparison with the real part (a) and the imaginary part (b) of $u(L,z)$ for NLOTM in the range step $\tau = 1/8$ (solid line) and ALOTM solution in Zhu and Li (2007) in the range step $\tau = 1/128$ (bold points) in Example 1

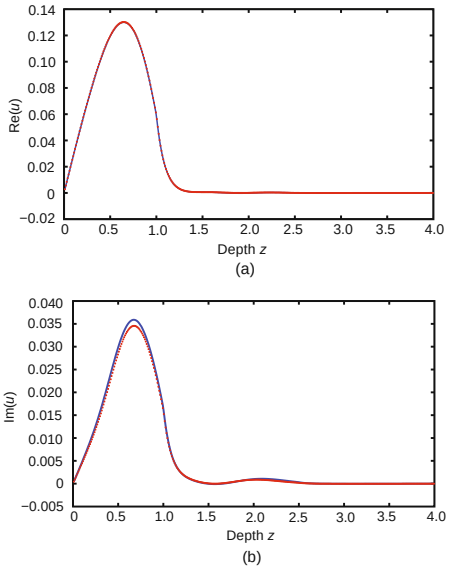

Fig. 4 Comparison with the real part (a) and the imaginary part (b) of $u(L,z)$ by NLOTM with $\delta = 0.05$ (bold points) and $\delta = 0.025$ (solid line) in the range step $\tau = 1/8$ in Example 1

$h_1(x) = 1 - \varepsilon_1 \exp(-\sigma_1(x/L - 0.5)^2)$, $h_2(x) = H - \varepsilon_2 \exp(-\sigma_2(x/L - 0.48)^2)$, $\varepsilon_1 = \varepsilon_2 = 0.1$, $\sigma_1 = \sigma_2 = 10$, $0 \leqslant z \leqslant 1.5$, $0 \leqslant x \leqslant 10$.

Here, $u(0, \hat{z})$ is given by the eigenfunction whose corresponding eigenvalue is the third largest one at $x = L$ (Fig. 7). The corresponding solution is as shown in Fig. 8.

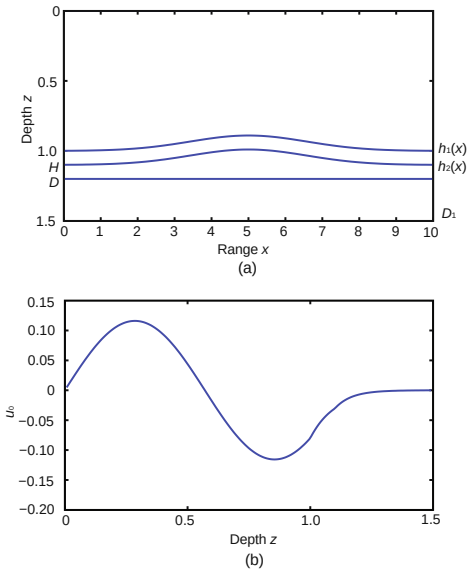

Fig. 5 Sketch map of the waveguide (a) and $u(0,z)$ (b) in Example 2

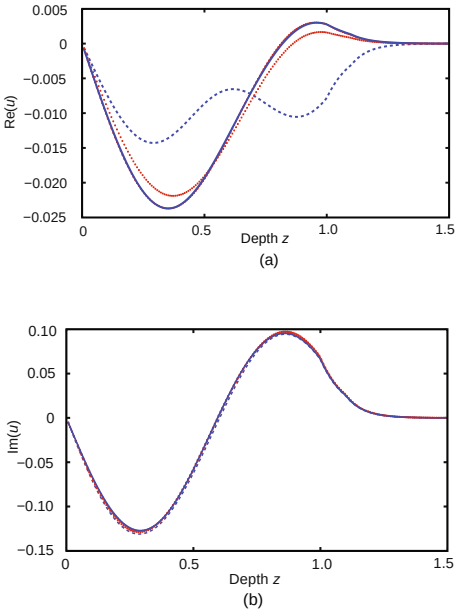

Fig. 6 Comparison with the real part (a) and the imaginary part (b) of $u(L,z)$ for $\tau = 1/8$ (dashed line), $\tau = 1/16$ (bold points), $\tau = 1/32$ (dotted line), and $\tau = 1/128$ (solid line) by NLOTM in Example 2

Example 4 Let

$$\kappa = \begin{cases} 16, & 0 < z < h_1(x), \\ 0.7 \times 16, & h_1(x) < z < h_2(x), \\ 0.2 \times 16, & h_2(x) < z < D_1, \end{cases}$$

with L=10, n=30, H=1.1, D=1.2, D_1=1.5, N=200, ρ_1=1, ρ_2=1.7, ρ_3=2.7, $h_1(x)$=$1-\varepsilon_1\exp(-\sigma_1(x/L-0.5)^2)$, $h_2(x) = H-\varepsilon_2\exp(-\sigma_2(x/L-0.5)^2)$, $\varepsilon_1 = \varepsilon_2 = 0.11$, $\sigma_1 = \sigma_2 = 10$, $0 \leqslant z \leqslant 1.5$, $0 \leqslant x \leqslant 10$.

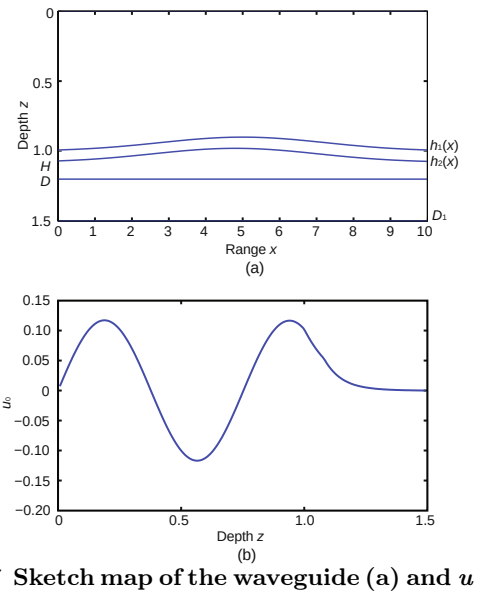

Fig. 7 Sketch map of the waveguide (a) and $u(0,z)$ (b) in Example 3

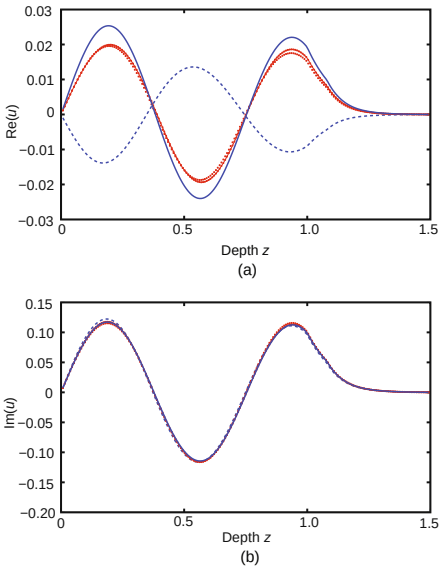

Fig. 8 Comparison with the real part (a) and the imaginary part (b) of $u(L,z)$ for $\tau = 1/8$ (dashed line), $\tau = 1/16$ (bold points), $\tau = 1/32$ (dotted line), and $\tau = 1/128$ (solid line) by NLOTM in Example 3

Here, $u(0,\hat{z})$ is given by the eigenfunction whose corresponding eigenvalue is the second largest one at $x = L$ (Fig. 9). The corresponding solution is as shown in Fig. 10.

In Examples 2–4, four different values for the time-steps are considered and the corresponding numerical results are presented together in Figs. 6, 8, and 10 for comparison. As shown by these figures,

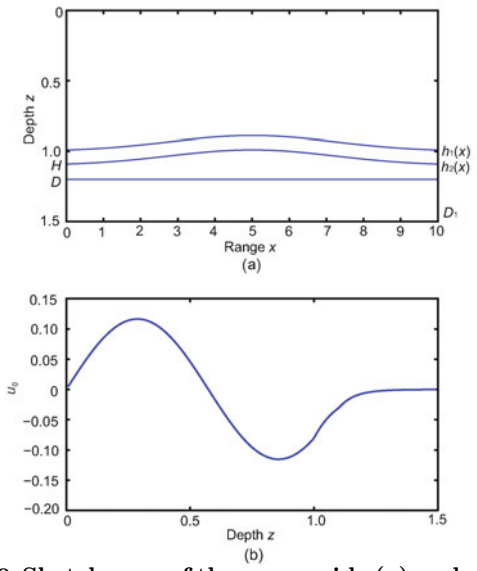

Fig. 9 Sketch map of the waveguide (a) and $u(0,z)$ (b) in Example 4

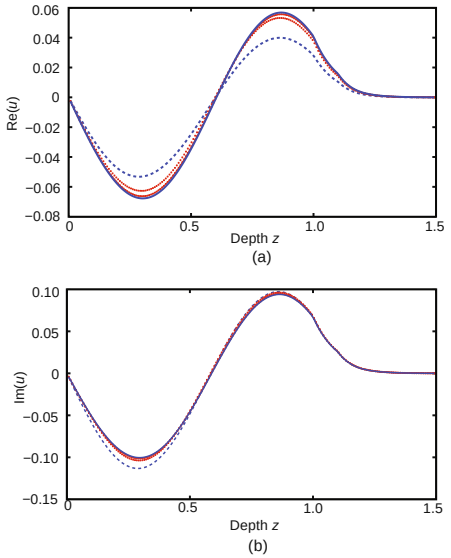

Fig. 10 Comparison with the real part (a) and the imaginary part (b) of $u(L,z)$ for $\tau = 1/8$ (dashed line), $\tau = 1/16$ (bold points), $\tau = 1/32$ (dotted line), and $\tau = 1/128$ (solid line) by NLOTM in Example 4

the solutions obtained with $\tau = 1/8$ are not reasonably accurate, while the solutions with $\tau = 1/16$ fit closely the more accurate solutions obtained with $\tau = 1/32$ and $\tau = 1/128$, at least similar to the shape of the waveforms. The figures indicate that reasonable NLOTM solutions are not obtained with the range step $\tau = 1/8$ like the numerical examples solved by the ALOTM in Zhu and Li (2007; 2008). The reason is that the waveguides with indivisible interfaces are generally more irregular. In fact, for the waveguides under the divisible assumption, the result in Example 1 shows that the NLOTM solution with $\tau = 1/8$ is a very close approximation to the 'exact' ALOTM solution. The solutions obtained with $\tau = 1/128$ act as the 'exact' solution. We compute the relative errors of $u(L,z)$ in the range step $\tau = 1/16$ and they are 0.0238, 0.0513, and 0.0491, respectively. The numerical examples show that good approximate solutions can be obtained by selecting quite large steps.

7 Discussions

The presupposition that there is a horizontal line between two adjoint interfaces is essential for the analytical local orthogonal transform method (ALOTM), which is used to compute wave propagation in multilayered waveguides. Our current study develops a practical numerical scheme for computing wave propagation in slowly varying acoustic waveguides without imposing the divisible assumption. The proposed numerical local orthogonal transform method (NLOTM) can be implemented with the marching processing and is generally more computationally efficient than the methods built on modified Schwarz-Christoffel mapping (Andersson, 2008; 2009) for large-scale range-dependent waveguides. This method is particularly useful for solving long-range wave propagation problems in slowly varying waveguides with multilayered medium structure. Numerical examples show that our method is feasible for solving the Helmholtz equation in slowly varing stratified waveguides using a large range step.

In an approximate comparison of the numerical Examples 2–4 with Example 1, we find that the convergence speed of Examples 2–4 using the NLOTM without meeting the divisible assumption is slower. Part of the reason lies in the irregularity of the computing domain in Examples 2–4 where the very close distance of two adjoint interfaces results in implementing the marching method in a relatively small range step. Furthermore, several problems for the NLOTM should be proposed and addressed for future studies:

1. In the coordinate transform, how to eliminate the side effects caused by the computing of the numerical partial derivatives? Since the considered waveguides are slowly varied, this gives rise to smoothing the computed data by some regulariza-

tion methods (Cullum, 1971) to smoothly reformulate the functions such as $x = m(\hat{x}, \hat{z}), z = n(\hat{x}, \hat{z})$, and $W(x, z)$ at $\hat{x} = \hat{x}_j$.

2. How to adaptively select optimal varying range steps of marching according to the characteristics of bottom or interfaces, and to eliminate the errors arising in the marching progress when the curved interfaces or boundaries become sharp abruptly?

3. In the traditional ALOTM, additional interfaces are introduced, which leads to the imposition of additional interface conditions. Thus, the corresponding effects of the additional interfaces and the problem of how to improve the additional interface conditions need to be investigated in future research.

References

Abrahamsson, L., Kreiss, H.O., 1994. Numerical solution of the coupled mode equations in duct acoustic. *J. Comput. Phys.*, **111**(1):1-14. [doi:10.1006/jcph.1994.1038]

Andersson, A., 2008. A modified Schwarz-Christoffel mapping for regions with piecewise smooth boundaries. *J. Comput. Appl. Math.*, **213**(1):56-70. [doi:10.1016/j.cam.2006.12.025]

Andersson, A., 2009. Modified Schwarz Christoffel mappings using approximate curve factors. *J. Comput. Appl. Math.*, **233**(4):1117-1127. [doi:10.1016/j.cam.2009.09.006]

Cullum, J., 1971. Numerical differentiation and regularization. *SIAM J. Numer. Anal.*, **8**(2):254-265. [doi:10.1137/0708026]

Delillo, T., Isakov, V., Valdivia, N., Wang, L., 2001. The detection of the source of acoustical noise in two dimensions. *SIAM J. Appl. Math.*, **61**(6):2104-2121. [doi:10.1137/S0036139900367152]

Fishman, L., 1993. One-way wave propagation methods in direct and inverse scalar wave propagation modeling. *Radio Sci.*, **28**(5):865-876. [doi:10.1029/93RS01632]

Fishman, L., Gautesen, A.K., Sun, A.K., 1997. Uniform high-frequency approximations of the square root Helmholtz operator symbol. *Wave Motion*, **26**:127-161. [doi:10.1016/S0165-2125(97)00018-8]

Jensen, F.B., Kuperman, W.A., Porter, M.B., Schmidt, H., 1994. Computational Ocean Acoustics. American Institute of Physics, New York.

Jin, B.T., Marin, L., 2008. The plane wave method for inverse problems associated with Helmholtz-type equations. *Eng. Anal. Bound. Elem.*, **32**(3):223-240. [doi:10.1016/j.enganabound.2007.08.005]

Jin, B.T., Zheng, Y., 2006. A meshless method for some inverse problems associated with the Helmholtz equation. *Comput. Methods Appl. Mech. Eng.*, **195**:2270-2288. [doi:10.1016/j.cma.2005.05.013]

Larsson, E., Abrahamsson, L., 1998. Parabolic Wave Equation versus the Helmholtz Equation in Ocean Acoustics. *In*: DeSanto, J.A. (Ed.), Mathematics and Numerical Aspects of Wave Propagation. SIAM, Philadelphia, p.582-584.

Lee, D., Pierce, A.D., 1995. Parabolic equation development in recent decade. *J. Comput. Acoust.*, **3**(2):95-173. [doi:10.1142/S0218396X95000070]

Li, P., Chen, Z.H., Zhu, J.X., 2008. An operator marching method for inverse problems in range dependent waveguides. *Comput. Methods Appl. Mech. Eng.*, **197**(49-50):4077-4091. [doi:10.1016/j.cma.2008.04.001]

Lu, Y.Y., 1999. One-way large range step methods for Helmholtz waveguides. *J. Comput. Phys.*, **152**(1):231-250. [doi:10.1006/jcph.1999.6243]

Lu, Y.Y., McLaughlin, J.R., 1996. The Riccati method for the Helmholtz equation. *J. Acoust. Soc. Am.*, **100**(3):1432-1446. [doi:10.1121/1.415990]

Lu, Y.Y., Huang, J., McLauphilin, J.R., 2001. Local orthogonal transformation and one-way methods for acoustics waveguides. *Wave Motion*, **34**(2):193-207. [doi:10.1016/S0165-2125(00)00083-4]

Marin, L., 2005. A meshless method for the numerical solution of the Cauchy problem associated with three-dimensional Helmholtz-type equations. *Appl. Math. Comput.*, **165**(2):355-374. [doi:10.1016/j.amc.2004.04.052]

Marin, L., Elliott, L., Heggs, P.J., Ingham, D.B., Lesnic, D., Wen, X., 2003. Conjugate gradient-boundary element solution to the Cauchy problem for Helmholtz-type equations. *Comput. Mech.*, **31**:367-372. [doi:10.1007/s00466-003-0439-y]

Nilsson, B., 2002. Acoustic transmission in curved ducts with varying cross-sections. *Proc. R. Soc. A*, **458**(2023):1555-1574. [doi:10.1098/rspa.2001.0910]

Tarppet, F.D., 1977. The Parabolic Approximation Method. *In*: Keller, J.B., Papadakis, J.S. (Eds.), Wave Propagation and Underwater Acoustics: Lecture Notes in Physics. Springer-Verlag, Berlin New York, **70**:224-287. [doi:10.1007/3-540-08527-0]

Zhu, J.X., Li, P., 2007. Local orthogonal transform for a class of acoustic waveguide. *Progr. Nat. Sci.*, **17**:18-28.

Zhu, J.X., Li, P., 2008. Mathematical treatment of wave propagation in acoustic waveguides with n curved interfaces. *J. Zhejiang Univ.-Sci. A*, **9**(10):1463-1472. [doi:10.1631/jzus.A0720064]

Zhu, J.X., Lu, Y.Y., 2002. Large range step method for acoustic waveguide with two layer media. *Progr. Nat. Sci.*, **12**:820-825.